Science of the Total Environment 572 (2016) 1025–1032

Contents lists available at ScienceDirect

Science of the Total Environment

journal homepage: www.elsevier.com/locate/scitotenv

Analysis of the improvement of selenite retention in smectite by adding alumina nanoparticles

Natalia Mayordomo *, Ursula Alonso, Tiziana Missana

CIEMAT, Department of Environment, Avenida Complutense 40, CP 28040, Madrid, Spain

HIGHLIGHTS

- Selenite sorption in smectite is significantly improved by adding γ-Al_2O_3 nanoparticles.
- Mixtures with 20 wt% of γ-Al_2O_3 approach the sorption capacity of pure alumina.
- Selenite sorption in mixtures is additive.
- Smectite/γ-Al_2O_3 heteroaggregation does not have strong effects on selenite sorption in mixtures.

GRAPHICAL ABSTRACT

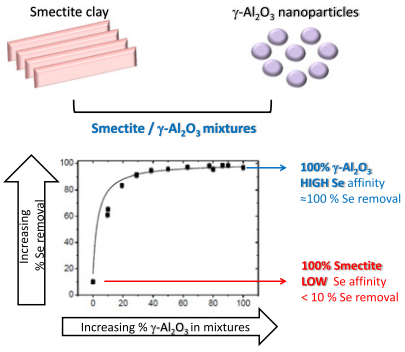

ARTICLE INFO

Article history:
Received 20 May 2016
Received in revised form 28 July 2016
Accepted 2 August 2016
Available online 5 August 2016

Editor: Kevin V. Thomas

Keywords:
Selenite
Sorption modeling
Mixtures
Smectite
Alumina

ABSTRACT

Smectite clay is used as barrier for hazardous waste retention and confinement. It is a powerful material to retain cations, but less effective for retaining anionic species like selenite. This study shows that the addition of a small percentage of γ-Al_2O_3 nanoparticles to smectite significantly improves selenite sorption. γ-Al_2O_3 nanoparticles provide high surface area and positively charged surface sites within a wide range of pH, since their point of zero charge is at pH 8–9. An addition of 20 wt% of γ-Al_2O_3 to smectite is sufficient to approach the sorption capacity of pure alumina. To analyze the sorption behavior of the smectite/oxide mixtures, a nonelectrostatic surface complexation model was considered, accounting for the surface complexation of $HSeO_3^-$ and SeO_3^{2-}, the anion competition, and the formation of surface ternary complexes with major cations present in the solution. Selenite sorption in mixtures was satisfactorily described with the surface parameters and complexation constants defined for the pure systems, accounting only for the mixture weight fractions. Sorption in mixtures was additive despite the particle heteroaggregation observed in previous stability studies carried out on smectite/γ-Al_2O_3 mixtures.

1. Introduction

Some anions present in aquatic environment, such as fluoride, bromate, phosphate, sulfate, nitrite, nitrate, selenite, and selenate, are hazardous for living organisms and ecosystems. Selenium is classified as a carcinogenic toxic that can lead to the development of some liver and kidney diseases (Banuelos et al., 2014; WHO, 2011). Selenium not only occurs naturally in the environment, but it is also emitted from its increasing use in electronics and fertilizers. Selenium concentrations found in contaminated sites range from 3 $\mu \cdot L^{-1}$ to 33 $mg \cdot L^{-1}$, where higher concentrations are generally related to mining wastewaters (Santos et al., 2015). Among all selenium oxidation states, Se(IV) is the most stable selenium aqueous species under moderate redox

* Corresponding author.
E-mail address: natalia.mayordomo@ciemat.es (N. Mayordomo).

http://dx.doi.org/10.1016/j.scitotenv.2016.08.008
0048-9697/

potential and neutral pH conditions, being mainly found as selenious acid (H_2SeO_3), hydrogen selenite ($HSeO_3^-$), or selenite (SeO_3^{2-}) (Séby et al., 2001).

Environmental protection agencies worldwide have claimed to develop more efficient, eco-friendly, and cost-effective remediation technologies for selenite removal. Several different methods have been developed to remove selenite from wastewater (Moore and Mahmoudkhani, 2011; WHO, 2011). A recent review on selenium remediation options highlights the advantages of sorption strategies and the potential of different adsorbents such as clays, oxides, and hydroxides. Reported selenite retention capacities varied from 0.6 to 833 $mg \cdot g^{-1}$, but the comparison of different systems is not straightforward, because the values depend on the water chemical conditions (pH and composition), initial selenium concentration, and the amount and properties of the selected adsorbent (Santos et al., 2015).

Pollutant confinement requires, in many cases, the use of materials that meet other characteristics besides contaminant retention, such as permeability, buffer ability, and swelling or sealing properties, which are fulfilled by clay minerals. Smectite clays are widely used for remediation purposes and in the disposal and storage of hazardous species such as nuclear waste (Pusch et al., 2015), because of their unique physicochemical properties, availability, and low cost.

Clay mineral structure determines its ability to retain contaminants on the surface (Grim, 1962). Smectite is a 2:1 type clay that has a permanent negative charge, with high capacity to retain cations, but anions to a lower extent. Previous sorption studies of selenite on smectite (Kim et al., 2012; Missana et al., 2009; Montavon et al., 2009; Peak, 2006; Shi et al., 2014) indicate that selenium retention is low and limited to a narrow pH range, where positively charged surface sites exist.

An additional material, with higher sorption ability and adequate surface properties, can be incorporated to improve the sorption capacity of smectite. Metal oxides such as iron oxides (Duc et al., 2006; Jang et al., 2015; Jordan et al., 2013; Kim et al., 2012), titanium oxide (Benedicto et al., 2013; Shi et al., 2009), and aluminum oxides (Boyle-Wight et al., 2002; Elzinga et al., 2009; Jegadeesan et al., 2003; Kumar et al., 2014; Missana et al., 2014; Papelis, 1995; Peak, 2006) are suitable candidates to retain selenium.

This study aims to analyze experimentally whether selenite retention on smectite clay is improved by the addition of γ-Al_2O_3 nanoparticles. Few studies deal with the anion adsorption on binary systems including clays (Behnsen and Riebe, 2008; Dousova et al., 2009; Hsu et al., 2008; Li and Bowman, 2001; Matusik, 2014; Mockovciaková et al., 2010; Peak, 2006; Riebe et al., 2001). To the best of our knowledge, no previous studies have proposed the addition of γ-Al_2O_3 to smectite to improve selenite retention.

We have selected γ-Al_2O_3, a metal oxide whose amphoteric behavior allows it to bind anions and cations depending on the pH (Dzombak and Morel, 1990). Its high point of zero charge (pH_{PZC} 8–9) broadens the pH range, where positively charged surface sites are available to retain anions. Furthermore, γ-Al_2O_3 nanoparticles have high surface area (>100 $m^2 \cdot g^{-1}$), which favors contaminant retention. Sorption of cationic species could be improved mainly in alkaline conditions; however, in acidic conditions, the dominant sorption mechanism would be cation exchange on smectite.

The surface properties of smectite and γ-Al_2O_3 mixture may, in principle, enhance anion sorption, but the observed stability behavior of smectite/γ-Al_2O_3 mixtures could affect the sorption ability of the mixture. Particle heteroaggregation was clearly observed when smectite and γ-Al_2O_3 coexisted (Mayordomo (in preparation); Mayordomo et al., 2014). The increase in the mean particle size may in fact lead to lower surface area available and lower surface sites available for sorption. To date, it has not been probed whether the mixture of γ-Al_2O_3 and smectite, which favors particle aggregation, affects the surface properties and therefore their sorption capacity. The effects on other smectite properties should also be verified.

Thus, the aims of this study are to analyze if the addition of γ-Al_2O_3 improves selenite sorption and to verify whether sorption in mixtures can be described using the surface parameters and complexation constants obtained for the pure systems by just considering their corresponding proportions.

Analyzing whether sorption in a mixed system is additive is not trivial, and has been scarcely treated (Palmer et al., 1981). A system is expected to be additive when either components do not interact or the interaction does not affect the surface properties. Nevertheless, we cannot rule out smectite/γ-Al_2O_3 interaction, because the addition of γ-Al_2O_3 to smectite (and vice versa) causes heteroaggregation of the particles, even under chemical conditions in which pure smectite and γ-Al_2O_3 are stable (Mayordomo (in preparation); Mayordomo et al., 2014).

Different models have been proposed to simulate selenite sorption on Al_2O_3 and clays (Goldberg, 2014, 2013; Morel et al., 2015), but we decided to use a simple model based on two previous studies, in which selenite sorption was studied on pure smectite (Missana et al., 2009) and γ-Al_2O_3 (Missana et al., 2014). Selected models have been updated including the contribution of major anions and cations present in solution.

Sorption in binary systems is complex, and ions present in solution may play a relevant role, either competing for the sorption sites (Galamboš et al., 2015; Hsu et al., 2008; Li et al., 1998; Moore and Young, 2005; Ochs et al., 2002; Rahnemaie et al., 2007; Su and Puls, 2001; Tuutijärvi et al., 2012; Villalobos et al., 2001; Xi et al., 2011) or favoring the anion sorption under alkaline conditions, if surface ternary complexes with multivalent cations are formed (Fein, 2002; Sumner, 1999).

The mechanistic description of selenite sorption in the binary system can assess whether the surface properties of both systems are affected by the observed heteroaggregation. On the contrary, if sorption behavior in the mixtures can be explained with the individual components, the overall description of contaminant retention in natural media, composed by complex mixtures of clay minerals and oxides, could be significantly simplified.

2. Materials and methods

2.1. Materials

2.1.1. Sorbents

Smectite was obtained from FEBEX bentonite, extracted from Cortijo de Archidona in Almería (Spain). Complete characterization of FEBEX clay can be found elsewhere (Huertas et al., 2000). For sorption experiments, the clay was purified to obtain the smectite fraction and homoionized in Na by dialysis, as described in Missana et al. (2009). Cation exchange capacity (CEC) of this smectite is CEC = 102 ± 4 meq/100 g, and its N_2-BET specific area is 33 $m^2 \cdot g^{-1}$.

Aluminum oxide nanoparticles (γ-Al_2O_3) with nominal diameter < 50 nm and N_2-BET specific surface area of 136 $m^2\ g^{-1}$ were selected (Aldrich). Their point of zero charge is pH_{pzc} = 8.3. Characterization of these nanoparticles and the study of their stability have been described elsewhere (Missana et al., 2014).

For sorption experiments, smectite and γ-Al_2O_3 were suspended in $NaClO_4$ at different ionic strengths (from 1×10^{-3} to 5×10^{-1} M). Different mixtures of smectite and alumina were prepared at fixed solid concentration (0.5 $g \cdot L^{-1}$) and ionic strength by varying their weight fractions.

Experiments were carried out under atmospheric conditions. Chemical analysis of contact electrolytes was carried out after 7 days of equilibrium. Major anions present in solution, under our experimental conditions, are ClO_4^-, Cl^-, and HCO_3^-. Concentration of ClO_4^- is fixed by the electrolyte concentration, Cl^- mainly originates from the addition of selenium tracer and pH adjustment with HCl, up to $[Cl^-] \approx 1 \times 10^{-3}$ M. The hydrogen carbonate results

from atmospheric CO_2 and smectite impurities, and its concentration varied from 25 to 80 mg·L^{-1}; the maximum value was considered for calculations. Major cation present in solution is Na, because the experiments are carried out in $NaClO_4$. The second most abundant cation in solution is Ca in the case of smectite ([Ca] ≈ 5×10^{-4} M) and Al^{3+} in the case of γ-Al_2O_3. Maximum Al^{3+} measured in solution was 6×10^{-4} M at pH 3, which corresponds to a γ-Al_2O_3 dissolution of <3%.

2.1.2. Adsorbate

Radioactive ^{75}Se was used for sorption experiments (Isotope Products). It is stored in a stock solution in 0.1 M HCl, including Na_2SeO_3 carrier. Its half-life is 119.8 days and its gamma emission can be detected at 136 and 256 keV. In sorption experiments, selenium activity in solution was detected by γ-counting with a NaI detector (Packard Auto-gamma COBRA 2).

When high selenium concentrations were required, stable selenium was added (Na_2SeO_3 purchased from Aldrich and prepared in 0.1 M HCl).

2.2. Se(IV) sorption experiments

Sorption experiments were performed under atmospheric conditions and at room temperature with a total solid concentration of 0.5 g·L^{-1}. This solid-to-liquid ratio is the same as that used in previous sorption experiments carried out on both materials separately (Missana et al., 2014, 2009). At low solid-to-liquid ratios, higher sorption capacities are achieved (when full saturation is not reached), while sorption efficiencies (expressed in %) are higher when more sorbent is used.

Suspensions were placed in 12-mL polypropylene centrifuge tubes, and ^{75}Se was added at the desired selenium concentration (1×10^{-10} to 1×10^{-3} M). After the addition of the radionuclide, the pH was readjusted, if necessary, with HCl or NaOH (1×10^{-2} to 1 M).

Previous studies on the kinetics of selenite sorption indicate that selenium sorption in smectite is nearly constant after 4–5 days of contact time (Missana et al., 2009), and very fast (<30 min) in γ-Al_2O_3. To ensure sorption equilibrium, all samples were continuously stirred for 7 days.

Sorption edges were carried out, as a function of pH (3 − 11), on pure smectite (100S) and γ-Al_2O_3 (100 A) and on mixtures of different Na-smectite/γ-Al_2O_3 weight fraction ratios (%): 90S/10A, 50S/50A, and 20S/80A. Ionic strength was set at 1×10^{-2} or 1×10^{-1} M in $NaClO_4$. Selenium concentration was [Se] ≈ 1.5×10^{-8} M.

To maintain pH constant over time, buffer solutions at 4×10^{-3} M were used as follows: acetic acid for pH 4.5, MES (2-(N-morpholino) ethane-sulfonic acid) for pH 5.5 and 6.0, MPS (3-(N-morpholino) propanesulfonic acid) for pH 6.5 and 7.0, TRIS (tris(hydroxymethyl)aminomethane) for pH 7.5 and 8.05, and CHES (3-(cyclohexyl amino)ethanesulfonic acid) for pH 9 and 10. It was previously verified that buffer addition below 1×10^{-2} M did not affect selenite sorption (Missana et al., 2009).

Sorption isotherms were carried out in γ-Al_2O_3 at pH 8 in 1×10^{-1} M $NaClO_4$, with varying selenium concentration from 1×10^{-10} to 1×10^{-3} M.

The sorption behavior of mixtures is analyzed in detail at pH where the maximum selenite sorption was achieved. Eight mixtures, at different weight fractions, were prepared in 1×10^{-1} M $NaClO_4$ at pH 4.5 and with a selenite concentration of 4×10^{-8} M.

After stirring, the tubes were centrifuged at 21,500 *g* for 1 h. This centrifugation ensures the deposition of particles with diameter > 10 nm.

After solid separation, three aliquots of the supernatant (2 mL) were sampled to measure selenium activity in solution.

Selenium distribution coefficients (K_d) for the solid and liquid phases were calculated as follows:

$$K_d = \frac{C_i - C_f}{C_f}\frac{V}{m} \quad (1)$$

where K_d is the distribution coefficient (mL·g^{-1}), C_i is the initial selenite concentration (Bq·mL^{-1}), C_f is the final selenite concentration (Bq·mL^{-1}), V is the suspension volume (mL), and m is the mass of sorbent (g).

Selenite sorption onto the centrifuge tubes was checked and was found to be almost negligible (<1%).

2.3. Sorption modeling

We aim to verify whether selenium sorption in smectite/γ-Al_2O_3 mixtures can be described with the surface complexation models developed for the individual systems.

Solid dissolution and selenite precipitation were enabled in the model. Al^{3+} hydrolysis was taken into account, considering the equilibrium constants reported in Thoegen et al. (2014). The concentration of Cl^-, ClO_4^-, and HCO_3^- and Na^+, Ca^{2+}, and Al^{3+} measured in solution were considered in speciation and sorption calculations. Formation of selenite solids with major cations present in solution was accounted for. The thermodynamic data used for selenium aqueous and solid species are presented in Table 1 (Séby et al., 2001).

Selenium sorption in both Na-smectite (Missana et al., 2009) and γ-Al_2O_3 (Missana et al., 2014) was previously described by considering a nonelectrostatic surface complexation model.

Smectite is a 2:1 layer clay, in which octahedral aluminum sheets are arranged between two tetrahedral silicon layers (Grim, 1962). In the tetrahedral and octahedral sheets, isomorphic substitutions impart a permanent negative charge, which can be neutralized by countercation adsorption onto the basal surfaces. This permanent charge provides the clay with CEC. Additionally, clays have surface hydroxylated sites (SOH) on the broken edges, similar to those present on the oxide surfaces, as γ-Al_2O_3, with a pH-dependent contribution to the surface charge (Sposito et al., 1999; Stumm, 1992). In both clays and oxides, surface complexation at SOH surface sites is expected to be the most relevant sorption process for anions.

Only one type of surface site was considered in both materials. Surface sites (SOH) are protonated and deprotonated with solution pH changes as follows:

$$SOH + H^+ \overset{K_+}{\Leftrightarrow} SOH_2^+ \quad (2)$$

Table 1
Thermodynamic selenium data included in the model. Data obtained from Séby et al. (2001) and Thoegen et al. (2014).

Species	Definition	logK
Aqueous		
$HSeO_3^-$	1 SeO_3[2−], 1 H[+]	8.40
H_2SeO_3	1 SeO_3[2−], 2 H[+]	11.08
Na_2SeO_3(aq)	1 SeO_3[2−], 2 Na[+]	0.02
$CaSeO_3$(aq)	1 SeO_3[2−], 1 Ca[2+]	3.17
Solid		
$Al_2(SeO_3)_3$	3 SeO_3[2−], 2 Al[3+]	32.47
$Na_2(SeO_3)$	1 SeO_3[2−], 2 Na[+]	3.51
Downeyite-Se	1 SeO_3[2−], 2 H[+], −1 H_2O	6.75
$SeCl_4$	1 SeO_3[2−], 6 H[+], 4 Cl[−], −3 H_2O	−14.44
$CaSeO_3$:2H_2O	1 SeO_3[2−], 1 Ca[2+], 2 H_2O	5.44
$CaSeO_3$:H2O	1 SeO_3[2−], 1 Ca[2+], 1 H_2O	7.76
$CaSeO_3$(s)	1 SeO_3[2−], 1 Ca[2+]	7.65

$$SOH \overset{K_-}{\Leftrightarrow} SO^- + H^+ \quad (3)$$

where K_+ and K_- are the protonation and deprotonation equilibrium constants, respectively.

The surface complexation of two selenium aqueous species ($HSeO_3^-$ and SeO_3^{2-}) on positively charged SOH_2^+ sites was initially considered:

$$SOH_2^+ + SeO_3^{2-} \overset{K_1}{\Leftrightarrow} SOH_2SeO_3^- \quad (4)$$

$$SOH_2^+ + HSeO_3^{2-} \overset{K_2}{\Leftrightarrow} SOH_2HSeO_3 \quad (5)$$

As mentioned earlier, we reviewed the previous model, incorporating the competition, or contribution, of major anions and cations present in solution.

Under alkaline conditions, pH-dependent surface sites are expected to be mainly negatively charged (SO^-). However, nonzero anion sorption is observed on soils and clays in alkaline conditions (Goldberg and Glaubig, 1988; Missana et al., 2009; Montavon et al., 2009). It has been observed that the presence of exchangeable cations lowers the solubility of certain anions, because they co-precipitate or bond together to mineral surfaces by forming surface ternary complexes (Sumner, 1999).

In this study, we incorporated surface ternary complexes (Fein, 2002), in which the cation bridges the negative charges of the surface and favors the coadsorption of selenite. At alkaline pH, surface sites are negatively charged and anion sorption would be unexpected, but Na^+ and Ca^{2+} promote the coadsorption of selenite. It is considered that the formation of ternary complexes is subjected to the ability to form soluble complexes and to the cation/anion ratio (Sumner, 1999), being favored when cation concentration is in relative excess to the anion one (Fein, 2002); this occurred in our case: cations (1×10^{-4} to 1×10^{-1} M)/selenite (1×10^{-8} to 1×10^{-10} M). The following equations were considered:

$$SO^- + Na^+ + SeO_3^{2-} \overset{K_3}{\Leftrightarrow} SO{-}Na{-}SeO_3{}^{2-} \quad (6)$$

$$SO^- + Ca^{2+} + SeO_3^{2-} \overset{K_4}{\Leftrightarrow} SO{-}Ca{-}SeO_3{}^- \quad (7)$$

Moreover, anions are expected to compete among themselves for the sorption sites (Galamboš et al., 2015; Hsu et al., 2008; Li et al., 1998; Moore and Young, 2005; Ochs et al., 2002; Rahnemaie et al., 2007; Su and Puls, 2001; Tuutijärvi et al., 2012; Villalobos et al., 2001; Xi et al., 2011). Anion complexation constants on the γ-Al_2O_3 surface were determined by Missana et al. (2014) for HCO_3^-, NO_3^-, SO_4^{2-}, and ClO_4^-. In the present study, we additionally determine the competition of Cl^-. The following equations were included in the selenium complexation model:

$$SOH_2^+ + HCO_3^- \overset{K_5}{\Leftrightarrow} SOH_2HCO_3 \quad (8)$$

$$SOH_2^+ + ClO_4^- \overset{K_6}{\Leftrightarrow} SOH_2ClO_4 \quad (9)$$

$$SOH_2^+ + Cl^- \overset{K_7}{\Leftrightarrow} SOH_2Cl \quad (10)$$

where K_i with $i = 5, 6$, and 7 are the anion complexation equilibrium constants on positively charged sites on the γ-Al_2O_3 surface.

No anion competition was considered in the case of smectite, because experimental results suggested that their contribution was negligible. Permanent negative charge exhibited by the clay reduces the approach of anions.

The surface complexation constants and solid parameters used to describe selenite sorption on smectite and γ-Al_2O_3 are listed in Table 2.

Table 2
Surface complexation equilibria and solid properties of smectite (Missana et al., 2009) and γ-Al_2O_3 (Missana et al., 2014). *Constant obtained in this study.

Parameter	γ-Al_2O_3	Na-smectite
CEC(meq/100 g)	-	102
N_2-BET ($m^2 \cdot g^{-1}$)	136	33
[SOH] Sites ($\mu eq \cdot m^{-2}$)	1.10	1.82
Equation	logK	logK
$SOH + H^+ \Leftrightarrow SOH_2^+$	6.90	5.30
$SOH - H^+ \Leftrightarrow SO^-$	−9.70	−8.40
$SOH_2^+ + SeO_3^{2-} \Leftrightarrow SOH_2SeO_3^-$	13.30	11.95
$SOH_2^+ + HSeO_3^- \Leftrightarrow SOH_2HSeO_3$	21.60	17.65
$SOH_2^+ + HCO_3^- \Leftrightarrow SOH_2HCO_3$	11.50	-
$SOH_2^+ + ClO_4^- \Leftrightarrow SOH_2ClO_4$	8.50	-
$SOH_2^+ + Cl^- \Leftrightarrow SOH_2Cl$	9.20*	-
$SO^- + SeO_3^{2-} + Na^+ \Leftrightarrow SO{-}Na{-}SeO_3{}^{2-}$	−5.2*	−4.0*
$SO^- + SeO_3^{2-} + Ca^{2+} \Leftrightarrow SO{-}Ca{-}SeO_3{}^-$	−0.2*	−0.2*

The geochemical code CHESS v.4 (van der Lee and de Wint, 1999) was used for the model description.

3. Results and discussion

Selenite sorption behavior was first analyzed on individual systems. Fig. 1a presents selenium distribution coefficients measured on Na-smectite, as a function of pH, at different ionic strengths (data from (Missana et al., 2009)), and Fig. 1b shows selenium sorption edges measured on γ-Al_2O_3 at different ionic strengths (1×10^{-2} to 1×10^{-1} M), with low ([Se] = 1.6×10^{-8} M) or high ([Se] = 9.6×10^{-6} M) selenium concentration. Data obtained under different experimental conditions are shown to facilitate process identification and to verify the goodness of the proposed models. In both systems, selenite sorption is the maximum at acidic pH, decreasing as pH increases, which is in agreement to sorption trend of anionic species. Comparatively, selenite sorption is clearly lower in Na-smectite (maximum log K_d = 2.65 mL·g^{-1}), than in γ-Al_2O_3, which exhibited much higher selenite retention, from acidic pH (maximum log K_d of 5 mL·g^{-1}) up to pH 10. In both cases, nonzero selenite sorption is observed under alkaline conditions, with a similar average log $K_d \approx 2$ mL·g^{-1}.

In the first attempt, selenite sorption was modeled considering surface complexation of $HSeO_3^-$ and SeO_3^{2-} (Eqs. (4) and (5)), and fits are plotted as dashed lines in the figures. On smectite, this model perfectly fits selenite sorption up to pH 8, but underestimates the observed selenium sorption at higher pH (Fig. 1a). In the case of γ-Al_2O_3 (Fig. 1b), it overestimates retention within pH 6–8 and underestimates retention for pH > 10.

As explained in the modeling section, the sorption model was modified, assuming the formation of selenite ternary complexes with Na^+ (Eq. (6)) and, when present in solution, also with Ca^{2+} (Eq. (7)). Anion competition was considered in the case of γ-Al_2O_3 (Eqs. (8)–(10)). The revised models are plotted as solid lines in the figures. Selected complexation constants for both γ-Al_2O_3 and Na-smectite are presented in Table 2. The incorporation of ternary selenite complexes accounts for the nonzero sorption measured at alkaline pH, as can be appreciated in Fig. 1.

The inclusion of anion competition in γ-Al_2O_3 clearly improved the fit (plotted as solid lines in Fig. 1b). HCO_3^- competition is especially relevant to explain the decreased selenite sorption for pH > 6. Fig. 2 presents selenium sorption isotherm measured at pH 8.2 on γ-Al_2O_3. The improved model is plotted as solid lines by taking into account the anion competition and selenium surface ternary complexes. It can be appreciated that the anion competition is relevant within a wide range of selenite concentrations (from 1×10^{-10} to 1×10^{-3} M).

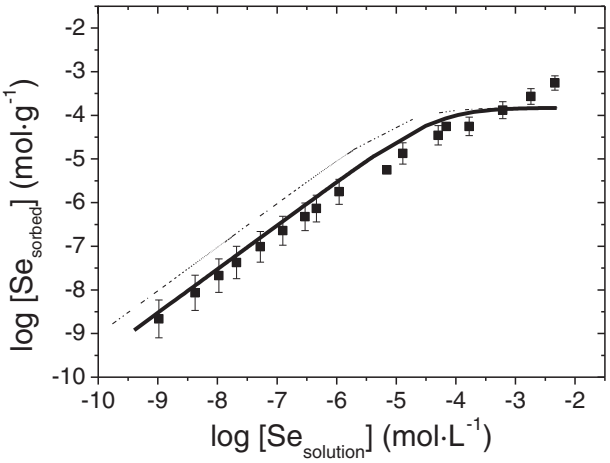

Fig. 2. Selenite sorption isotherm obtained in γ-Al_2O_3 at pH 8.2 in $NaClO_4$ (1×10^{-1} M). Solid-to-liquid ratio, 0.5 g·L^{-1}. Dashed lines represent the model considering surface complexation of $HSeO_3^-$ and SeO_3^{2-} and solid lines show the model including anion competition and Na^- and Ca-SeO_3^{2-} ternary complexes. Se concentration ranges from 10^{-10} up to 10^{-3} M.

Precipitation was neither experimentally observed under experimental conditions nor predicted by the model.

The model used to describe selenite sorption in both Na-smectite and γ-Al_2O_3 was the same, but selenite and hydrogen selenite complexation constants were higher in alumina than in smectite (Table 2), because of the higher selenite affinity toward alumina.

Once sorption models for the independent systems were defined, selenite sorption in Na-smectite (S)/γ-Al_2O_3 (A) mixtures was analyzed. Fig. 3 presents selenium sorption edges measured on mixtures at different weight fractions (90S/10A and 50S/50A), in comparison to those measured on Na-smectite (100S) and γ-Al_2O_3 (100 A). Selenite sorption in mixtures is significantly higher than that in smectite, indicating that the addition of γ-Al_2O_3 nanoparticles improves selenite retention. The sorption trend in the mixtures is similar to that observed on pure systems, in which maximum sorption is reached at acidic pH (pH ≈ 4.5) and sorption decreases as pH increases, because the number of positively charged sites decreases. Adding only a small amount of γ-Al_2O_3 to Na-smectite (10% in weight) results in approximately 12 times higher distribution coefficient in the whole range of experimental pH. At acidic pH, log K_d increases from 2.5 to 3.6 mL·g^{-1} with 10% of γ-Al_2O_3 and up to 4.5 mL·g^{-1} with a 50% addition. In the pH region between 6 and 8, sorption is also improved, despite the competition of HCO_3^- binding to alumina sites; the value of log K_d increases from 2.2 to 3.2 mL·g^{-1}

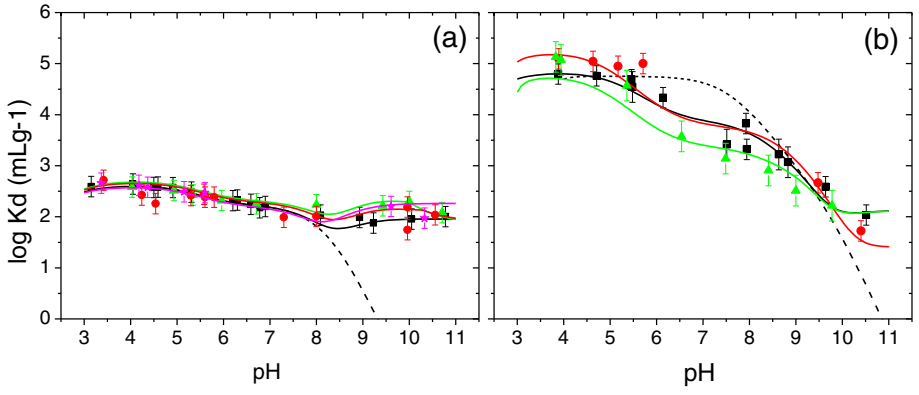

Fig. 1. (a) Sorption edges for selenite onto Na-smectite in $NaClO_4$ at different ionic strengths: (▲) 1×10^{-3} M, (●) 1×10^{-2} M, (■) 1×10^{-1} M, and (★) 5×10^{-1} M, with [Se] = 4×10^{-10} M and solid-to-liquid ratio 0.5 g·L^{-1}. **(b)** Sorption edges for selenite onto 0.5 g·L^{-1} of γ-Al_2O_3 in $NaClO_4$ at different ionic strengths: (●) 1×10^{-2} M and (■) 1×10^{-1} M with [Se] = 1.6×10^{-8} M and (▲) 1×10^{-1} M with [Se] = 9.6×10^{-5} M. Dashed lines correspond to the fits considering surface complexation of $HSeO_3^-$ and SeO_3^{2-} and solid lines correspond to the improved model, including the formation of ternary Na- and Ca-SeO_3^{2-} and anion competition.

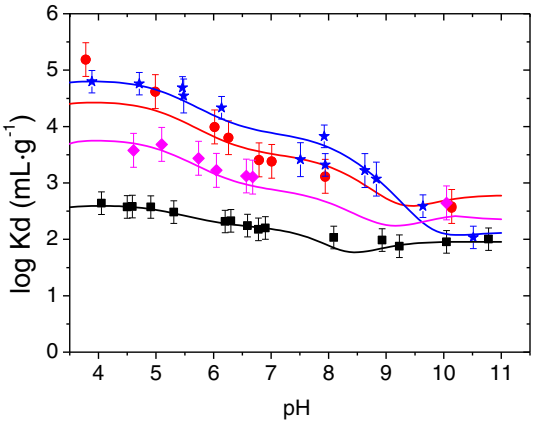

Fig. 3. Selenium sorption edges measured in 1×10^{-1} M $NaClO_4$ in different systems: (■) 100% Na-smectite; (◆) 90% Na-smectite/10% γ-Al_2O_3 (●) 50% Na-smectite/γ-50% Al_2O_3, and (★) 100% γ-Al_2O_3. Total solid concentration was 0.5 g·L^{-1} and [Se] = 4×10^{-8} M. Simulations are plotted as solid lines (complexation constants present in Table 2).

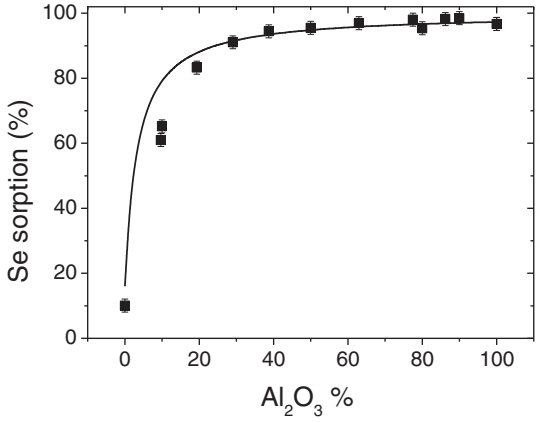

Fig. 4. Selenium sorption (%) increase in Na-smectite as a function of γ-Al_2O_3 nanoparticles addition. Total solid concentration was 0.5 g·L^{-1} in 1×10^{-1} M $NaClO_4$ and [Se] = 4×10^{-8} M. Simulations carried out with parameters presented in Table 2 are plotted as solid lines.

with a 10% γ-Al_2O_3, and with 50% addition, it approaches the value achieved on 100% γ-Al_2O_3 (log K_d = 4 mL·g^{-1}). At pH higher than the pH_{pzc} of γ-Al_2O_3, selenite sorption in Na-smectite and γ-Al_2O_3 is similar the retention is explained by ternary complexes with cations present in solution; in this region, selenite sorption is slightly higher in both mixtures, most probably due to Ca traces caused by smectite additionally contributing to retain selenium on the alumina surface.

One of the aims of this study was to verify if the sorption behavior of mixtures could be described by using surface complexation models defined for the independent systems. As shown in Fig. 3, selenite sorption behavior in mixtures (plotted as solid lines) is perfectly described with the parameters obtained for the pure minerals (Table 2), within the whole pH range and at different ionic strengths, and by considering only the correspondent weight fraction of mixture component. This indicates that selenite sorption is additive.

Some studies also showed sorption additivity, for example, in mixed clays (Missana et al., 2009); but other studies pointed out the complexity of sorption behavior in mixed systems. For example, uranium sorption on mixed Ti and Fe oxide phases was lower than expected and did not behave in an additive manner (Comarmond et al., 2012). The additivity of systems suggests limited interaction between the two components. We have observed that the coexistence of Na-smectite and γ-Al_2O_3 induced particle aggregation, even in those pH regions where electrostatic attraction was unexpected (Mayordomo et al., 2014). However, the fact that selenite sorption in mixtures was described considering the surface parameters of the individual system contribution indicates that particle heteroaggregation, with a noticeable increase in the mean particle diameter (Mayordomo et al., 2014), does not affect the sorption capacity of the mixture.

In all cases, the maximum selenite sorption is attained at pH ≈ 4.5; therefore, we analyze the effect of mixture fraction under these conditions. Fig. 4 presents selenite sorption measured at pH 4.5 in Na-smectite with the increasing load of alumina. By increasing the amount of alumina, Se sorption in smectite is enhanced. At lower alumina weight fractions (0.5–10)%, sorption is significantly improved from a 10% selenite retention up to 60%, with an alumina addition of <20 wt%. Moreover, selenium retention in mixtures with an alumina content of >20 wt%. resembles the sorption power of pure γ-Al_2O_3. Selenite sorption in mixtures is satisfactorily predicted by considering the individual models (Fig. 4).

Anion sorption is subjected to the availability of positively charged surface sites (SOH_2^+). The amount of positively charged sites available to bind selenite changes according to the mixture composition, and can be calculated by considering the surface equations and parameters included in Table 2. Fig. 5 shows the total concentration (μM) of positive sites (SOH_2^+) and the individual contributions of Na-smectite and γ-Al_2O_3, referred to the % of Al_2O_3 in the mixture (from 0% to 100%). Calculations were performed considering the experimental conditions (solid concentration of 0.5 g·L^{-1}, in $NaClO_4$ 1×10^{-1} M at pH 4.5). The available surface sites are directly related to the materials' surface area, which is higher in alumina. Positive surface sites show a linear increase with increasing γ-Al_2O_3 amount (Fig. 5), providing additional sites to retain anions such as selenite. Positively charged sites of Na-smectite prevails over alumina ones when alumina fraction is <25%.

It was shown that γ-Al_2O_3 significantly improves selenite sorption in smectite. Selenium sorption capacities calculated under the experimental conditions (0.5 g·L^{-1} and [Se] = 4×10^{-8} M) indicated that by adding γ-Al_2O_3 to smectite, sorption capacity is increased from 4 to 12 mg·g^{-1}. With the surface complexation model that we had developed, we estimated selenium sorption capacities under equivalent selenium and sorbent concentrations reported by Santos et al. (2015), and the maximum sorption values predicted in our model, at acidic conditions, were in the upper range reported.

Mixture behavior indicates that the independent surfaces are still available to interact with the selenite (or other) hazardous species. A small amount of γ-Al_2O_3 nanoparticles provided sufficient surface edge sites, therefore, the mixture behaves as pure γ-Al_2O_3 to what

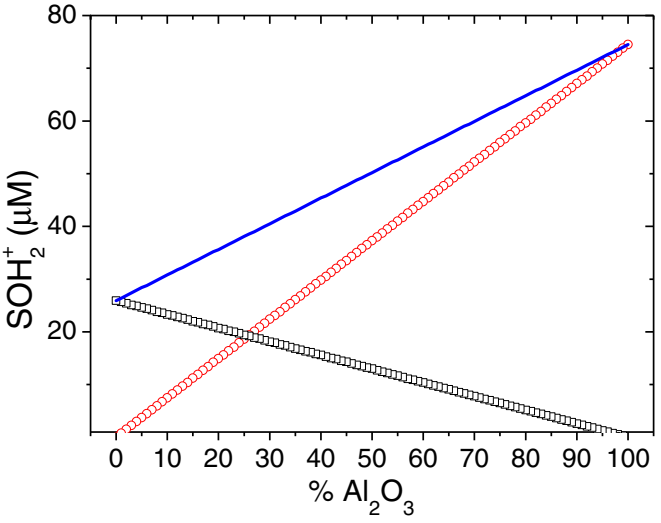

Fig. 5. Positive surface sites available in mixtures with varying content of γ-Al_2O_3 at pH 4.5. (—) Total SOH_2 +; (□) Smectite SOH_2^+; and (○) γ-Al_2O_3 SOH_2^+.

concerns sorption. This property allows designing suitable mixtures for a specific scenario of pollution, in which the content of γ-Al_2O_3 nanoparticles is minimized but attain maximum selenite removal.

4. Conclusions

It was experimentally shown that selenite retention in smectite is improved by adding γ-Al_2O_3 nanoparticles. The binary mixture enhanced selenite retention within all pH conditions. Under conditions where selenite retention is the maximum, an addition of 10% of γ-Al_2O_3 is sufficient to improve selenite retention from 10% to 60%. Selenite sorption in the pure systems was described considering complexation of selenite and hydrogen selenite and incorporating competition of anions present in solution. The formation of ternary selenite complexes with major cations in solution was also accounted for to explain the nonzero selenite sorption measured in alkaline conditions. Selenite sorption behavior in mixtures could be described with the surface parameters and complexation constants defined for the pure systems, showing that the sorption was additive. The proven sorption additivity indicates that the heteroaggregation exhibited by smectite/γ-Al_2O_3 mixtures does not affect their surface properties in terms of sorption capacity.

A small addition of γ-Al_2O_3 nanoparticles (20 wt% under experimental conditions) to smectite was sufficient to approach sorption capacity of pure γ-Al_2O_3. This allows to design suitable mixtures for a specific scenario of pollution, in which the γ-Al_2O_3 nanoparticle content is minimized but improves selenite removal.

Acknowledgments

This study was supported by MIRAME (CTM-2014-60482-P) Spanish Ministry of Economy and Competitiveness projects. N.M. acknowledges FPI BES-2012-056603 predoc grant from MINECO (Spain).

References

Banuelos, G.S., Lin, Z.-Q., Yin, X., 2014. Selenium in the Environment and Human Health. first ed. CRC Press Taylor & Francis Group, London, UK.
Behnsen, J., Riebe, B., 2008. Anion selectivity of organobentonites. Appl. Geochem. 23, 2746–2752. http://dx.doi.org/10.1016/j.apgeochem.2008.06.019.
Benedicto, A., Missana, T., Degueldre, C., 2013. Predictions of TiO_2-driven migration of Se(IV) based on an integrated study of TiO_2 colloid stability and Se(IV) surface adsorption. Sci. Total Environ. 449, 214–222. http://dx.doi.org/10.1016/j.scitotenv.2013.01.058.
Boyle-Wight, E.J., Katz, L.E., Hayes, K.F., 2002. Macroscopic studies of the effects of selenate and selenite on cobalt sorption to γ-Al_2O_3. Environ. Sci. Technol. 36, 1212–1218. http://dx.doi.org/10.1021/es001775a.
Comarmond, M.J., Payne, T.E., Collins, R.N., Palmer, G., Lumpkin, G.R., Angove, M.J., 2012. Inhibition of uranium(VI) sorption on titanium dioxide by surface iron(III) species in ferric oxide/titanium dioxide systems. Environ. Sci. Technol. 46, 11128–11134. http://dx.doi.org/10.1021/es302574j.
Dousova, B., Fuitova, L., Herzogova, L., Grycar, T., Kolousek, D., Machovic, V., 2009. Modified low-grade aluminosilicates as effective sorbents of hazardeous oxyanions from aqueous systems. Acta Geodyn. Geomater. 6, 193–200.
Duc, M., Lefèvre, G., Fédoroff, M., 2006. Sorption of selenite ions on hematite. J. Colloid Interface Sci. 298, 556–563. http://dx.doi.org/10.1016/j.jcis.2006.01.029.
Dzombak, D.A., Morel, F.M.M., 1990. Surface Complexation Modeling. Hydrous Ferric Oxide. first ed. John Wiley and Sons, Cambridge (United States).
Elzinga, E.J., Tang, Y., McDonald, J., DeSisto, S., Reeder, R.J., 2009. Macroscopic and spectroscopic characterization of selenate, selenite, and chromate adsorption at the solid-water interface of g-Al_2O_3. J. Colloid Interface Sci. 340, 153–159. http://dx.doi.org/10.1016/j.jcis.2009.08.033.
Fein, J.B., 2002. The effects of ternary surface complexes on the adsorption of metal cations and organic acids onto mineral surfaces. Water–Rock Interact. Ore Depos. Environ. Geochemistry A Tribut. to David A. Crerar. The Geochemical Soc. Spec. Publ. N7, pp. 365–378.
Galamboš, M., Daňo, M., Viglašová, E., Krivosudský, L., Rosskopfová, O., Novák, I., Berek, D., Rajec, P., 2015. Effect of competing anions on pertechnetate adsorption by activated carbon. J. Radioanal. Nucl. Chem. 1219–1224. http://dx.doi.org/10.1007/s10967-015-3953-4.
Goldberg, S., 2013. Modeling selenite adsorption envelopes on oxides, clay minerals, and soils using the triple layer model. Soil Sci. Soc. Am. J. 77, 64. http://dx.doi.org/10.2136/sssaj2012.0205.
Goldberg, S., 2014. Macroscopic experimental and modeling evaluation of selenite and selenate adsorption mechanisms on gibbsite. Soil Sci. Soc. Am. J. 78, 473–479. http://dx.doi.org/10.2136/sssaj2013.06.0249.
Goldberg, S., Glaubig, R.A., 1988. Anion sorption on a calcareous, Montmorillonitic soil—arsenic. Soil Sci. Soc. Am. J. 52, 1297. http://dx.doi.org/10.2136/sssaj1988.03615995005200050015x.
Grim, R.E., 1962. Applied Clay Mineralogy. second ed. Mc Graw-Hill, Toronto (Canada).
Hsu, J.C., Lin, C.J., Liao, C.H., Chen, S.T., 2008. Evaluation of the multiple-ion competition in the adsorption of As(V) onto reclaimed iron-oxide coated sands by fractional factorial design. Chemosphere 72, 1049–1055. http://dx.doi.org/10.1016/j.chemosphere.2008.03.060.
Huertas, F., Fuentes-Santillana, J.L., Jullien, F., Rivas, P., Linares, J., Fariña, P., Ghoreychi, M., Jockwer, N., Kickmaier, W., Martínez, M., Samper, J., Alonso, E., Elorza, F.J., 2000. FEBEX project final report. EUR 19147. Madrid (Spain).
Jang, M., Pak, S., Kim, M.-J., 2015. Comparison of adsorption characteristics of Se(IV) and Se(VI) onto hematite: effects of reaction time, initial concentration, pH, and ionic strength. Environ. Earth Sci. 74, 1169–1173. http://dx.doi.org/10.1007/s12665-015-4103-6.
Jegadeesan, G., Mondal, K., Lalvani, S.B., 2003. Comparative study of selenite adsorption on carbon based adsorbents and activated alumina. Environ. Technol. 24, 1049–1059. http://dx.doi.org/10.1080/09593330309385644.
Jordan, N., Ritter, A., Foerstendorf, H., Scheinost, A.C., Weiß, S., Heim, K., Grenzer, J., Mücklich, A., Reuther, H., 2013. Adsorption mechanism of selenium(VI) onto maghemite. Geochim. Cosmochim. Acta 103, 63–75. http://dx.doi.org/10.1016/j.gca.2012.09.048.
Kim, S.S., Min, J.H., Baik, M.H., Kim, G.N., Choi, J.W., 2012. Estimation of the behaviors of selenium in the near field of repository. Nucl. Eng. Technol. 44, 945–952. http://dx.doi.org/10.5516/NET.06.2012.010.
Kumar, E., Bhatnagar, A., Hogland, W., Marques, M., Sillanpää, M., 2014. Interaction of anionic pollutants with Al-based adsorbents in aqueous media – a review. Chem. Eng. J. 241, 443–456. http://dx.doi.org/10.1016/j.cej.2013.10.065.
Li, Z., Bowman, R.S., 2001. Retention of inorganic oxyanions by organo-kaolinite. Water Res. 35, 3771–3776. http://dx.doi.org/10.1016/S0043-1354(01)00120-8.
Li, Z., Anghel, I., Bowman, R.S., 1998. Sorption of oxyanions by surfactant-modified zeolite. J. Dispers. Sci. Technol. 19, 843–857. http://dx.doi.org/10.1080/01932699808913218.
Matusik, J., 2014. Arsenate, orthophosphate, sulfate, and nitrate sorption equilibria and kinetics for halloysite and kaolinites with an induced positive charge. Chem. Eng. J. 246, 244–253. http://dx.doi.org/10.1016/j.cej.2014.03.004.
Mayordomo, N., 2016. Heteroaggregation of alumina nanoparticles with smectite and its proportion effect. (in prep).
Mayordomo, N., Alonso, U., Missana, T., Benedicto, A., García-Gutiérrez, M., 2014. Addition of Al_2O_3 nanoparticles to bentonite: effects on surface charge and Cd sorption properties. MRS Proc. 1665, 131–137. http://dx.doi.org/10.1557/opl.2014.638.
Missana, T., Alonso, U., García-Gutiérrez, M., 2009. Experimental study and modelling of selenite sorption onto illite and smectite clays. J. Colloid Interface Sci. 334, 132–138. http://dx.doi.org/10.1016/j.jcis.2009.02.059.
Missana, T., Benedicto, A., Mayordomo, N., Alonso, U., 2014. Analysis of anion adsorption effects on alumina nanoparticles stability. Appl. Geochem. 49, 68–76. http://dx.doi.org/10.1016/j.apgeochem.2014.04.003.
Mockovciaková, A., Orolínová, Z., Skvarla, J., 2010. Enhancement of the bentonite sorption properties. J. Hazard. Mater. 180, 274–281. http://dx.doi.org/10.1016/j.jhazmat.2010.04.027.
Montavon, G., Guo, Z., Lützenkirchen, J., Alhajji, E., Kedziorek, M.A.M., Bourg, A.C.M., Grambow, B., 2009. Interaction of selenite with MX-80 bentonite: effect of minor phases, pH, selenite loading, solution composition and compaction. Colloids Surf. A Physicochem. Eng. Asp. 332, 71–77. http://dx.doi.org/10.1016/j.colsurfa.2008.09.014.
Moore, L., Mahmoudkhani, A., 2011. Methods for removing selenium from aqueous systems. Proceeding Tailings Mine Waste. Vancouver.
Moore, A.M., Young, T.M., 2005. Chloride interactions with iron surfaces: implications for perchlorate and nitrate remediation using permeable reactive barriers. J. Environ. Eng. 131, 924–933. http://dx.doi.org/10.1061/(ASCE)0733-9372(2005)131:6(924).
Morel, J.-P., Marmier, N., Hurel, C., Morel-Desrosiers, N., 2015. Thermodynamics of selenium sorption on alumina and montmorillonite. Cogent Chem. 1, 1–12. http://dx.doi.org/10.1080/23312009.2015.1070943.
Ochs, M., Lotenbhach, B., Giffaut, E., 2002. Uptake of oxo-anions formation: experimental evidence and modelling. Radiochim. Acta 90, 639–646. http://dx.doi.org/10.1524/ract.2002.90.9-11_2002.639.
Palmer, D.A., Shiao, S.Y., Meyer, R.E., Wethington, J.A., 1981. Adsorption of nuclides on mixtures of minerals. J. Inorg. Nucl. Chem. 43, 3317–3322. http://dx.doi.org/10.1016/0022-1902(81)80109-1.
Papelis, C., 1995. X-ray photoelectron spectroscopic studies of cadmium and selenite adsorption on aluminum oxides. Environ. Sci. Technol. 29, 1526–1533.
Peak, D., 2006. Adsorption mechanisms of selenium oxyanions at the aluminum oxide/water interface. J. Colloid Interface Sci. 303, 337–345. http://dx.doi.org/10.1016/j.jcis.2006.08.014.
Pusch, R., Kasbohm, J., Knutsson, S., Yang, T., Nguyen-Thanh, L., 2015. The role of smectite clay barriers for isolating high-level radioactive waste (HLW) in shallow and deep repositories. Procedia Earth Planet. Sci. 15, 680–687. http://dx.doi.org/10.1016/j.proeps.2015.08.084.
Rahnemaie, R., Hiemstra, T., van Riemsdijk, W.H., 2007. Carbonate adsorption on goethite in competition with phosphate. J. Colloid Interface Sci. 315, 415–425. http://dx.doi.org/10.1016/j.jcis.2007.07.017.

Riebe, B., Bors, J., Dultz, S., 2001. Retardation capacity of organophilic bentonite for anionic fission products. J. Contam. Hydrol. 47, 255–264. http://dx.doi.org/10.1016/S0169-7722(00)00154-6.

Santos, S., Ungureanu, G., Boaventura, R., Botelho, C., 2015. Selenium contaminated waters: an overview of analytical methods, treatment options and recent advances in sorption methods. Sci. Total Environ. 521-522, 246–260. http://dx.doi.org/10.1016/j.scitotenv.2015.03.107.

Séby, F., Potin-Gautier, M., Giffaut, E., Borge, G., Donard, O.F.X., 2001. A critical review of thermodynamic data for selenium species at 25 °C. Chem. Geol. 171, 173–194.

Shi, K., Wang, X., Guo, Z., Wang, S., Wu, W., 2009. Se(IV) sorption on TiO2: sorption kinetics and surface complexation modeling. Colloids Surf. A Physicochem. Eng. Asp. 349, 90–95. http://dx.doi.org/10.1016/j.colsurfa.2009.07.057.

Shi, K., Ye, Y., Guo, N., Guo, Z., Wu, W., 2014. Evaluation of Se(IV) removal from aqueous solution by GMZ Na-bentonite: batch experiment and modeling studies. J. Radioanal. Nucl. Chem. 299, 583–589. http://dx.doi.org/10.1007/s10967-013-2807-1.

Sposito, G., Skipper, N.T., Sutton, R., Park, S., Soper, A.K., Greathouse, J.A., 1999. Surface geochemistry of the clay minerals. Proc. Natl. Acad. Sci. U. S. A. 96, 3358–3364. http://dx.doi.org/10.1073/pnas.96.7.3358.

Stumm, W., 1992. Chemistry of the Solid-Water Interface. first ed. John Wiley and Sons, Toronto (Canada).

Su, C., Puls, R.W., 2001. Arsenate and arsenite removal by zerovalent iron: effects of phosphate, silicate, carbonate, borate, sulfate, chromate, molybdate, and nitrate, relative to chloride. Environ. Sci. Technol. 35, 4562–4568. http://dx.doi.org/10.1021/es010768z.

Sumner, M.E. (Ed.), 1999. Handbook of Soil Science. CRC Press.

Thoegen, T., Hummel, W., Berner, U., Curti, E., 2014. The PSI/Nagra Chemical Thermodynamic Database 12/07.

Tuutijärvi, T., Repo, E., Vahala, R., Sillanpää, M., Chen, G., 2012. Effect of competing anions on arsenate adsorption onto maghemite nanoparticles. Chin. J. Chem. Eng. 20, 505–514. http://dx.doi.org/10.1016/S1004-9541(11)60212-7.

van der Lee, J., de Wint, L., 1999. Chess Tutorial and Cookbook, Technical Repot LHM/RD/99/05.

Villalobos, M., Trotz, M.A., Leckie, J.O., 2001. Surface complexation modeling of carbonate effects on the adsorption of Cr(VI), Pb(II), and U(VI) on goethite. Environ. Sci. Technol. 35, 3849–3856.

WHO, 2011. Selenium in Drinking-water Background document for development of [WWW Document]. World Heal. Organ, Geneva (doi:WHO/HSE/WSH/10.01/14).

Xi, J., He, M., Lin, C., 2011. Adsorption of antimony(III) and antimony(V) on bentonite: kinetics, thermodynamics and anion competition. Microchem. J. 97, 85–91. http://dx.doi.org/10.1016/j.microc.2010.05.017.